Tetrahedron 68 (2012) 7502–7508

Contents lists available at SciVerse ScienceDirect

Tetrahedron

journal homepage: www.elsevier.com/locate/tet

Twisted bimesitylene-based oxadiazoles as novel host materials for phosphorescent OLEDs

Parthasarathy Venkatakrishnan[a], Palani Natarajan[a], Jarugu Narasimha Moorthy[a,*], Zhenghuan Lin[b], Tahsin J. Chow[b,*]

[a] Department of Chemistry, Indian Institute of Technology, Kanpur 208016, India
[b] Institute of Chemistry, Academia Sinica, Taipei, Taiwan 115, Republic of China

ARTICLE INFO

Article history:
Received 19 March 2012
Received in revised form 22 May 2012
Accepted 24 May 2012
Available online 31 May 2012

ABSTRACT

The D_{2d}-symmetric bimesitylene core has been exploited for designing novel host materials required in the construction of phosphorescence-based organic light emitting devices. The oxadiazole-functionalized *twisted* bimesitylenes are found to exhibit high band gap (triplet energies), and excellent glass transition temperatures and thermal stabilities for ready exploitation as host materials. The electron-transporting ability and respectable luminance efficiencies with triplet dopants (up to 19.0 cd/A) allow oxadiazole-functionalized bimesitylenes as promising materials for phosphorescence-based light emitting devices, namely PHOLEDs.

1. Introduction

Commercialization of flat-panel displays has gained importance due to the recent evolution in highly efficient phosphorescence-based organic light emitting diodes (PHOLEDs);[1] the internal quantum efficiencies of phosphorescent emitters can, in theory, reach 100% by harvesting both singlet and triplet excitons.[2] In recent years, several host emitting materials—polymers as well as small molecules—have been synthesized and reported to be efficient for use in PHOLEDs. The prerequisites for application of any material as a good host are: (i) higher triplet energy than that of the guest for efficient energy transfer,[3] (ii) good thermal and morphological stability, and (iii) appropriate energy level matching with the adjacent layers for efficient charge injection and recombination. Designing materials that satisfy all of the above conditions is a challenging task and enormous research is still in progress. The small molecule-based host materials explored for the purpose of electrophosphorescence include carbazoles,[2b,4] silanes,[5] phosphine oxides,[6] triazoles,[7] triazines,[8] quinolines,[9] triphenylamines,[10] transition metal ions,[11] etc. While bipolar host systems incorporating oxadiazole moiety have been reported in the literature,[12] only oxadiazole-based host materials are still rare.[13] Oxadiazoles are excellent electron-transporting/hole-blocking materials used in OLEDs due to their electron deficient nature.[14] Indeed, oxadiazole units advantageously restrict π-conjugation to afford materials with deeply lying highest occupied molecular orbitals (HOMOs) such that the triplet energies (E_Ts) are high.[15]

In continuation of our recent investigations on organic light emitting materials,[16] we envisaged the possibility of functionalizing *twisted* bimesitylene core with oxadiazoles to develop host materials for PHOLEDs, cf. **1** and **2**, Fig. 1.

It was anticipated a priori that (i) orthogonal orientation of the aryl rings of bimesitylene core would preclude close packing/aggregation in the solid state due to π–π stacking, (ii) the introduction of the oxadiazole moieties would enhance the electron-transporting properties across the layer and restrict π-conjugation to afford materials with wide band-gap energy (E_g) and high triplet energy (E_T), and (iii) the oxadiazoles with bulky substituents at the termini would permit excellent thermal and morphological stability of the devices. Herein, we describe synthesis, photophysical, thermal, and electrophosphorescence properties of novel bimesitylene-based oxadiazoles **1** and **2**. It is shown that the bimesitylene-based materials based on a rational design and substitution pattern do indeed serve as efficient electrophosphorescent materials.

2. Results and discussion

2.1. Synthesis of oxadiazole-functionalized bimesitylenes 1 and 2

Scheme 1 depicts the synthetic route for preparation of **1** and **2** based on Pd(0)-catalyzed Suzuki coupling reaction

---

* Corresponding authors. Tel.: +91 512 2597438; fax: +91 512 2597436 (J.N.M.); tel.: +886 2 27898552; fax: +886 2 27831237 (T.J.C.); e-mail addresses: moorthy@iitk.ac.in (J.N. Moorthy), tjchow@chem.sinica.edu.tw (T.J. Chow).

0040-4020/$ – see front matter © 2012 Elsevier Ltd. All rights reserved.
doi:10.1016/j.tet.2012.05.101

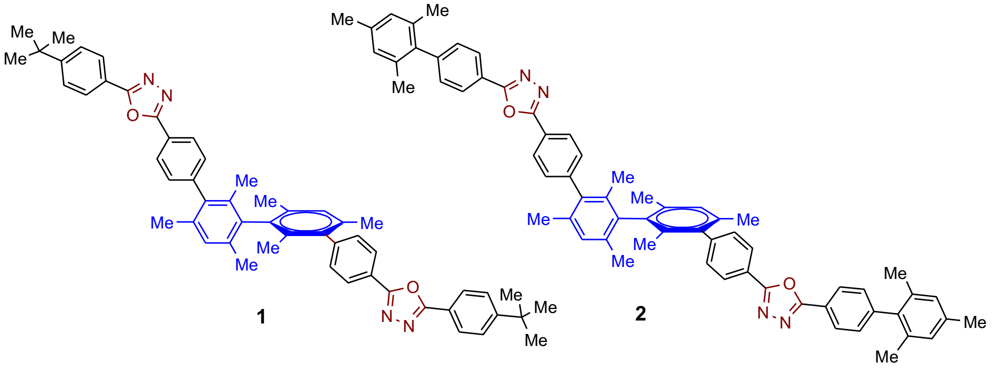

Fig. 1. Novel host materials **1** and **2** based on bimesitylenes.

between 3,3′-diiodobimesityl[16a] and 4-formylphenylboronic acid.[17] The dialdehyde thus obtained[16c] was subjected to oxidation using oxone[18] to afford the corresponding 3,3′-bis(4-carboxyphenyl)bimesityl. Reactions of the latter with thionyl chloride followed by treatment with suitably-functionalized tetrazoles led to oxadiazole-functionalized bimesitylenes **1** and **2** in excellent isolated yields (82–87%). Both compounds **1** and **2** were thoroughly characterized by ^{1}H, ^{13}C NMR spectroscopy, mass spectrometry, and elemental analysis, cf. Experimental section.

2.2. Photophysical properties

The UV–vis absorption and photoluminescence spectra of **1** and **2** in chloroform solution at room temperature are shown in Fig. 2 and the results are summarized in Table 1. The oxadiazole **1** is found to exhibit absorption maximum (λ_{max}) at 293 nm, while **2** shows at 298 nm. In a similar manner, the room temperature fluorescence spectrum of **2** displays emission maximum around 363 nm, which is red-shifted by 8 nm from that of **1**. The fluorescence lifetimes of **1** and **2** were determined to be 1.06 and 0.93 ns,

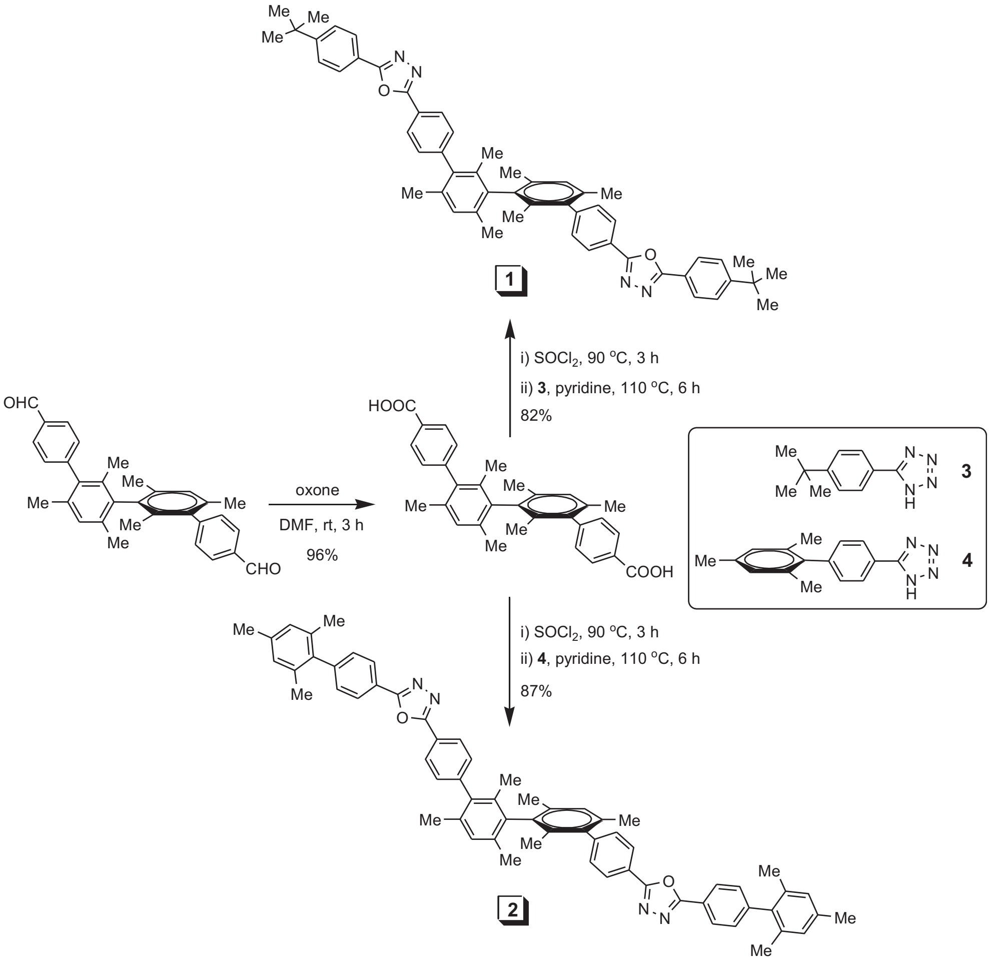

Scheme 1. Synthesis of the bimesitylene-based oxadiazoles **1** and **2**.

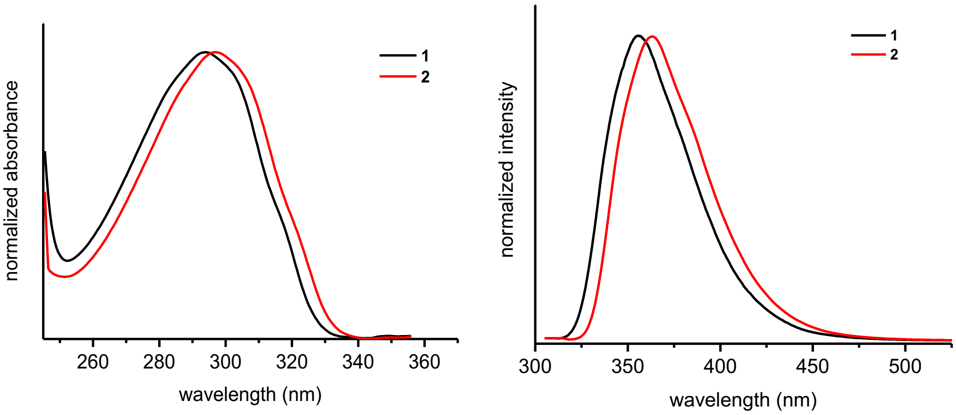

Fig. 2. UV–vis absorption (left) and photoluminescence (right) spectra for the oxadiazole-functionalized bimesitylenes **1** and **2** in chloroform.

respectively. A marginal bathochromic shift observed in both absorption and emission spectra of **2** may be attributed to the presence of the additional mesitylene unit in **2**, which presumably imparts weak π-communication due to the restricted rotation. It is well known that the oxadiazole restricts π-conjugation beyond the ring even if the rings were to be coplanar.[15] Similarity in both shape and pattern of the absorption as well as emission spectra of **1** and **2** attests to similar electronic behavior of the chromophoric moieties present in the two molecules.

As mentioned earlier, for a material to be a good host, it is necessary that it exhibits higher triplet energy than that of the phosphorescent emitter (dopant). This criterion benefits us with high efficiencies by arresting the back energy transfer from dopant to the host.[3] To gauge the triplet energies (E_T), the phosphorescence spectra for **1** and **2** were recorded at 77 K in 2-methyltetrahydrofuran. The spectra revealed a three-band pattern that is common to both (Table 1, see Supplementary data for details). It was on the basis of their longer lifetimes (2.45 µs for **2**; 0.71 (49%) and 4.53 (51%) µs for **1**) when compared to the fluorescence lifetimes (singlet) that the emission was attributed to that emanating from triplet states. The triplet energies for **1** and **2** were derived from the 0–0 transitions (highest energy vibronic peak) at ca. 462 nm, which corresponds to 2.68 eV. This value is comparatively higher than that of CBP[19] (4,4′-bis(*N*-carbazolyl)biphenyl, E_T=2.56 eV), a popular host material used for PHOLEDs, which attests to the utility of **1** and **2** as an appropriate host material for red and green phosphorescent emitters. Additionally, the E_T of **1**/**2** is sufficiently larger than the phosphorescent emitter $Ir(PPy)_3$[5a,19a,c] (tris(2-phenylpyridine)iridium(III), E_T=2.42 eV) for the triplet excitons to be confined. The HOMO energy levels for **1** (5.86 eV) and **2** (6.06 eV) were determined from the ultraviolet photoelectron spectroscopy and the LUMO energy level was deduced by subtracting the optical band gap energy (E_g) from the corresponding HOMO energy (Table 1); E_g was calculated in each case from the tail-end of the absorption spectrum.

The wide band-gap energy (singlet energy gap) of ca. 3.71 eV is expected for the oxadiazoles **1** and **2** due to their large triplet energy gap.[19a] Indeed, such materials with wide band gaps can in principle be used as hole-blocking/electron-transporting materials.[14]

2.3. Thermal properties

The thermal and morphological stabilities of **1** and **2** were examined by thermogravimetric and differential scanning calorimetric analyses, respectively. The bimesitylene-based oxadiazoles reveal excellent thermal stabilities as indicated by their high decomposition temperatures (T_d); T_ds measured at 5% weight loss for **1** and **2** are 431 and 449 °C, respectively (Fig. 3). Compound **1** exhibited glass transition temperature (T_g) around 173 °C and an endothermic melting temperature (T_m) at 302 °C, where as **2** displayed T_g around 182 °C with T_m at 316 °C (Table 1, Fig. 3). It is noteworthy that the T_gs for **1** and **2** are much higher than the popular and most often employed host materials, i.e., *m*-CP (T_g=60 °C) and CBP (T_g=62 °C).[19b] Also, it is important to mention that the glass transition temperatures of **1** and **2** are higher than those of the most popular oxadiazole-based electron-transporting materials, such as, 2-(4-biphenylyl)-5-(4-*tert*-butylphenyl)-1,3,4-oxadiazole (PBD, T_g=60 °C),[1b,14c] 1,3-bis[(4-*tert*-butylphenyl)-1,3,4-oxadiazolyl]phenylene (OXD-7, T_g=77 °C),[1b,14c,e] and are higher than the recently reported non-bipolar host-emitters that contain oxadiazoles (BOBP, T_g=45 °C; TPOs and PPOs, T_gs up to 121 °C).[13] The excellent thermal and morphological stability of our oxadiazoles may be attributed to the orthogonal arrangement of the rigid bimesitylene core. The attachment of additional mesitylene ring in the case of **2** contributes to

Table 1
Optical and thermal properties of the bimesitylene-based oxadiazoles **1** and **2**

Compound	λ_{abs}[a] (nm)	λ_{em}[a] (nm)	λ_{em}[b] (nm)	T_g,T_m,T_c[c] (°C)	T_d[d] (°C)	HOMO[e] (eV)	LUMO[f] (eV)	E_g[g] (eV)	E_T[h] (eV)
1	294	356	462, 497, 522	173, 302, 211	431	5.86	2.15	3.71	2.68
2	297	363	463, 497, 525	182, 316, —[i]	449	6.06	2.36	3.70	2.68

[a] Measured in chloroform solutions at room temperature.
[b] Measured in 2-methyltetrahydrofuran at 77 K.
[c] Determined from differential scanning calorimetric analyses performed under nitrogen at a heating rate of 10 °C/min; T_g—glass transition temperature, T_m—melting temperature, and T_c—crystallization temperature.
[d] Determined from thermogravimetric analyses performed under nitrogen at a heating rate of 10 °C/min; T_d—decomposition temperature.
[e] Derived from UVPES.
[f] Calculated by subtracting the optical band gap energy (E_g) from the corresponding HOMO energy.
[g] Calculated from the tail-end of the absorption spectrum.
[h] Derived from the 0–0 transitions of the phosphorescence spectrum.
[i] No T_c observed.

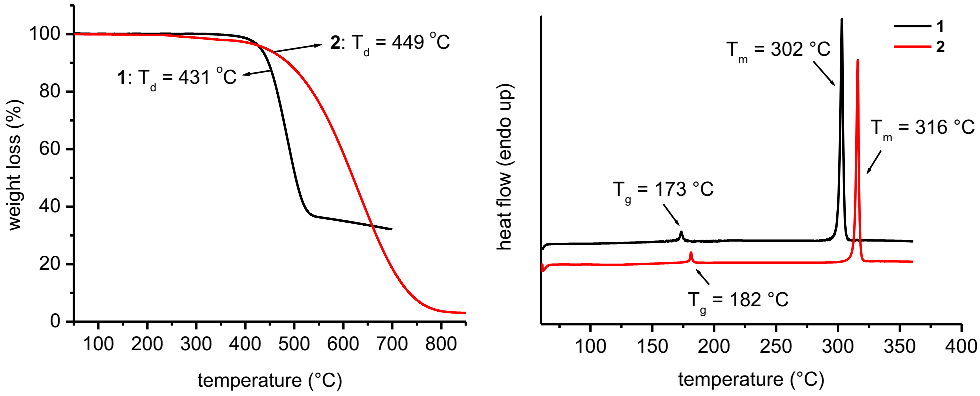

Fig. 3. Thermogravimetric (left) and differential scanning calorimetric (right) scans for oxadiazole-functionalized bimesitylenes **1** and **2**.

increase in the molecular size and rigidity of the system leading to better thermal properties. Such thermally/morphologically stable compounds permit fabrication of devices via vacuum sublimation without any decomposition.

2.4. Electroluminescence properties

The ability of oxadiazoles **1** and **2** to function in PHOLEDs as host materials was tested by fabricating devices with following configurations: (**A**) ITO/NPB (400 Å)/Ir(PPy)$_3$:**1** (6%, 400 Å)/Alq$_3$ (400 Å)/LiF (10 Å)/Al (1500 Å), (**B**) ITO/NPB (400 Å)/Ir(PPy)$_3$:**1** (6%, 400 Å)/LiF (10 Å)/Al (1500 Å), (**C**) ITO/NPB (400 Å)/Ir(PPy)$_3$:**1** (6%, 400 Å)/TPBI (400 Å)/LiF (10 Å)/Al (1500 Å), and (**D**) ITO/NPB (400 Å)/Ir(PPy)$_3$:**2** (6%, 400 Å)/TPBI (400 Å)/LiF (10 Å)/Al (1500 Å), where ITO (indium tin oxide) was the anode, NPB (*N*,*N*′-bisnaphthalen-1-yl)-*N*,*N*′-bis(phenyl)-benzidine) served as the hole-transporting layer, Ir(PPy)$_3$ acts as a dopant, and **1** or **2** as the host material, TPBI (2,2′,2″-(1,3,5-benzenetriyl)-tris(1-phenyl-1-*H*-benzimidazole) or Alq$_3$ (tris(8-hydroxyquinolinato)aluminum) as an electron-transporting (ET) layer, and LiF/Al as the composite cathode. The electrophosphorescence spectrum and the HOMO–LUMO energy level diagram for the devices **C** and **D** are provided in Fig. 4. The current–voltage–luminance characteristics (*I*–*V*–*L*) and current efficiency, power efficiency and quantum efficiency versus current density plots of the TPBI-based devices **A** and **D** are shown in Fig. 5. The device characteristics for all the PHOLED devices are compiled in Table 2.

First of all, the oxadiazole **1** was tested for electrophosphorescence using Alq$_3$—the most common electron-transporting material—as the ET layer (device **A**: ITO/NPB (400 Å)/Ir(PPy)$_3$:**1** (6%, 400 Å)/Alq$_3$ (400 Å)/LiF (10 Å)/Al (1500 Å)). This device **A** exhibited luminance and external quantum efficiencies of 4.6 cd/A and 1.4%, respectively. The poor efficiencies could be reasoned from the very proximate HOMO levels of Alq$_3$ (HOMO=6.0 eV, LUMO=3.3 eV; E_T=2.0 eV)[19a,20] and **1** (5.86 eV). Consequently, one may presume distribution of holes in both emitting (EM) and ET layers such that recombination of holes and electrons may occur in the two zones leading to an overall reduction in the electrophosphorescence efficiency (η_{ex}). Hence, it was deemed important to introduce a hole-blocking layer in combination with Alq$_3$ or to use ET materials with much higher LUMOs and higher triplet energies for effective confinement of holes and electrons as well as triplet excitons in the EM layer. As a next step, a simplified device configuration **B** was adopted, wherein the ET layer was totally eliminated from the device structure with an aim to probe the electron-transporting ability of the oxadiazole-based material in PHOLED device structure. The device **B** (ITO/NPB (400 Å)/Ir(PPy)$_3$:**1** (6%, 400 Å)/LiF (10 Å)/Al (1500 Å)) that does not contain any electron-transporting layer displayed better performance than the previous Alq$_3$-based device **A** with luminance and power efficiencies of 9.4 cd/A and 3.3 lm/W, respectively. In other words, the device **B** showed almost a two-fold increase in the device performance compared to that of device **A**. It is well known that oxadiazole derivatives act as good electron-transporting materials.[14c–e] One would expect that removal of the electron-transporting layer would result in electron injection difficult. However, the dual nature—electron-transport as well as hosting—of the oxadiazole-based molecular systems seemingly allow facile electron injection into the EM layer leading to EL emission as a consequence of immediate recombination with well-confined holes in EM layer to account for the observed two-fold enhancement of the efficiencies.

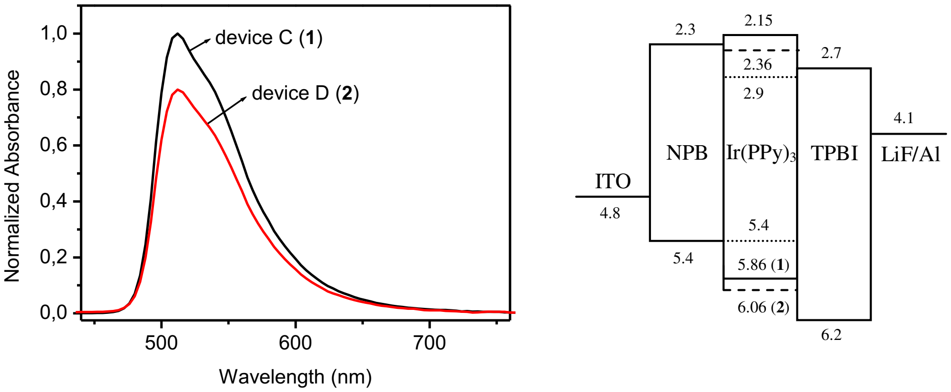

Fig. 4. The normalized electrophosphorescence spectrum (left) and the HOMO and LUMO energy level (eV) diagram for the devices **C** and **D**. In the emitting layer, solid line represents **1**, dashed line **2**, and the dotted line Ir(PPy)$_3$.

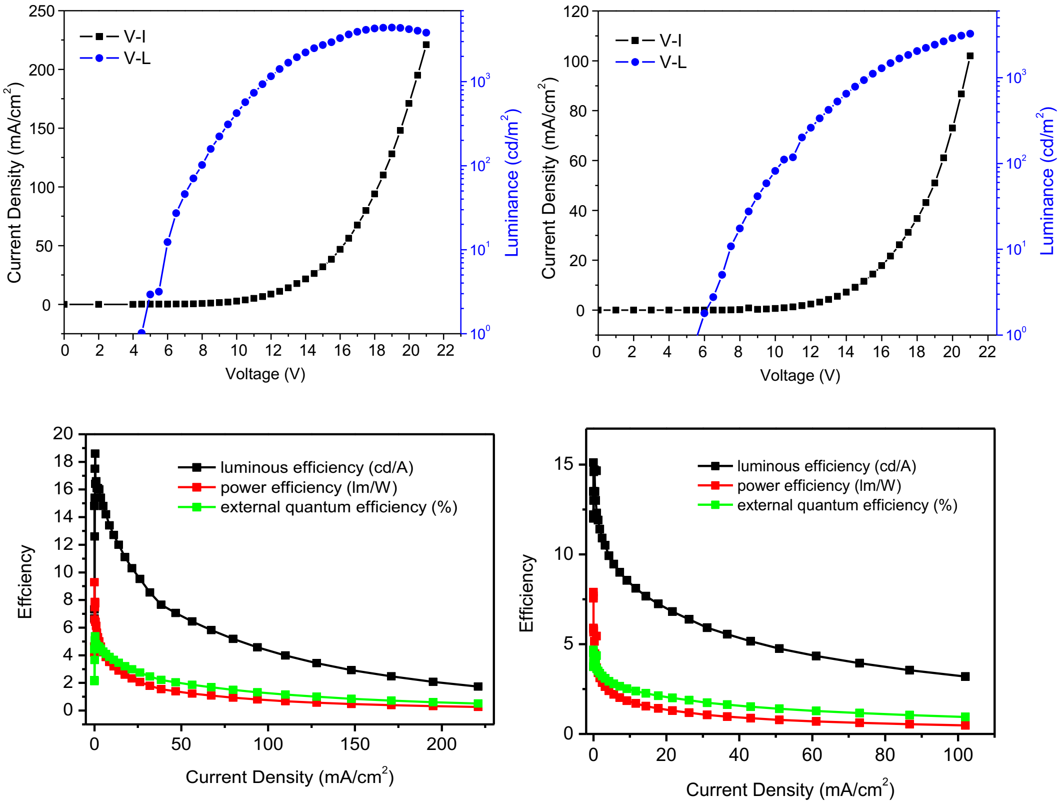

Fig. 5. The *I–V–L* characteristics (top), and luminous, power, external efficiencies versus current density (bottom) for the TPBI-devices of **1** (left) and **2** (right).

It must be emphasized that the materials that perform dual roles of electron transporting and hosting are in high demand, as they simplify the device construction. Although ETL materials have been tested as host-emitters in PHOLEDs, study on their dual nature is relatively less common.[13,19a,21] Due to the above-mentioned reasons, TPBI was introduced in place of Alq_3 as an electron-transporting material/hole-blocking material between the cathode and the emitting layer, as in the configuration of device **C** (ITO/NPB (400 Å)/$Ir(PPy)_3$:**1** (6%, 400 Å)/TPBI (400 Å)/LiF (10 Å)/Al (1500 Å)). As expected, **1** revealed maximum luminance efficiency of 18.6 cd/A, maximum power efficiency of 9.3 lm/W and maximum external quantum efficiency of 5.4% demonstrating superior performance under device C conditions. It is noteworthy that at a current density of 20 mA/cm^2 (13.8 V) the device exhibited a brightness of 2130 cd/m^2 with a luminance efficiency of 10.6 cd/A. Such an enhancement in the EL efficiencies of device **C** can be readily pointed to facile electron injection into the EM layer (barrier=0.55 eV) from the TPBI layer; with Alq_3, the electron-injection barrier is estimated to be 1.15 eV. The use of TPBI in place of Alq_3 reduces the electron-injection barrier considerably (0.6 eV). The advantage associated with TPBI is that it can be used both as an electron-transporting material as well as a hole-blocking material (HOMO=6.2 eV; LUMO=2.7 eV).[22] Evidently, qualities of TPBI that include higher lying LUMOs, wide band-gap energy and higher triplet energy (E_T=2.74 eV)[23] contribute to the enhancement of the device **C**. Thus, the performance of the TPBI-based device **C**, in general, was found to be superior when compared to the Alq_3-based device **A** and the device lacking ETL, i.e., **B**. Therefore, compound **2** was fabricated with a similar configuration as that of device **C**. The resultant device **D** for oxadiazole **2** exhibited respectable EL performance with maximum luminance and external quantum efficiencies 15.1 cd/A and 4.7%, respectively; the power efficiency for this device was found to be 7.9 lm/W. At a current density of 20 mA/cm^2, the luminance and external quantum efficiencies were found to be 7.0 cd/A and 2.1%, respectively. Despite the fact that $Ir(PPy)_3$ (HOMO=5.4 eV; LUMO=2.9 eV)[19c] possesses greater depth of 0.66 eV for trapping holes in the host **2** (than in **1**, 0.46 eV), the better EL device performance of device **C** than device **D** is probably due to the higher LUMO level of **1** for efficient electron trapping. In other words, the HOMO and LUMO levels of the host oxadiazole **1** that lie 0.46 eV below and 0.75 eV above those for $Ir(PPy)_3$, respectively, are crucial for trapping holes and electrons to form excitons effectively in the dopant sites. The dramatic increase in the turn-on voltage in device **D** could be attributed to the difficulty in charge injection due to the presence of bulky mesitylene units at the termini in the case of **2**. Otherwise, it is instructive to note that the performances of devices **C** and **D** are improved by 3–4 times when compared with those for the device **A**. The device efficiencies for **1** and **2** are indeed very comparable to other non-bipolar oxadiazole-based host-emitters, for example, BPBO,[13a] and TPOs and PPOs.[13b] Based on the color

Table 2
Device characteristics of PHOLEDs based on oxadiazoles

Device[a]	λ^{EL}_{max} (nm)	V_{on}[b]	η_l[c]	η_p[d]	η_{ex}[e]	L_{max}[f]	FWHM[g]	CIE[h] *x*, *y*
A	508	4.7	4.6	1.4	1.4	3326	56	0.26, 0.62
B	512	4.5	9.4	3.3	2.9	4493	64	0.28, 0.63
C	512	4.5	18.6	9.3	5.4	4397	72	0.30, 0.62
D	512	5.8	15.1	7.9	4.7	3254	64	0.29, 0.62

[a] The configurations of four devices are: (**A**) ITO/NPB (400 Å)/$Ir(PPy)_3$:**1** (6%, 400 Å)/Alq_3 (400 Å)/LiF (10 Å)/Al (1500 Å), (**B**) ITO/NPB (400 Å)/$Ir(PPy)_3$:**1** (6%, 400 Å)/LiF (10 Å)/Al (1500 Å), (**C**) ITO/NPB (400 Å)/$Ir(PPy)_3$:**1** (6%, 400 Å)/TPBI (400 Å)/LiF (10 Å)/Al (1500 Å), and (**D**) ITO/NPB (400 Å)/$Ir(PPy)_3$:**2** (6%, 400 Å)/TPBI (400 Å)/LiF (10 Å)/Al (1500 Å).

[b] Turn-on voltage (V).

[c] Maximum luminance efficiency (cd/A).

[d] Maximum power efficiency (lm/W).

[e] Maximum external quantum efficiency (%).

[f] Maximum luminance achieved (cd/m^2).

[g] Full-width at half-maximum from the EL spectrum.

[h] 1931 CIE chromaticity coordinates.

chromaticity diagram, the CIE coordinates of all these devices indicate a *yellowish-green* electrophosphorescence emission. Clearly, more experimentation entailing doping concentration and hole-transport as well as electron-transport materials with better matching of HOMO and LUMOs facilitating triplet-exciton confinement should lead to better device performance characteristics, and we are currently exploring these possibilities. Although presently observed results with minimum device experimentation are not readily comparable to some of the best results with oxadiazoles, they nonetheless emphasize the utility of bimesityl-based oxadiazoles as a new class of electron-transport-type host materials.

3. Conclusions

It is shown that bimesityl core can be exploited to develop host materials for phosphorescent light emitting diodes. The twofold oxadiazole-functionalized bimesitylenes **1** and **2** are shown to display significantly high glass transition temperatures, thermal stabilities and permit vacuum sublimation as a means for the construction of devices. The functional (electron-transporting as well as hosting) behavior of these materials has been demonstrated by fabricating yellowish-green-emitting electrophosphorescent devices that exhibit luminance efficiencies as high as 18.6 cd/A. Clearly, the bimesityl scaffold allows rational design and functionalization to produce materials of varying properties for application in OLEDs, and we are endeavoring to develop new materials based on this design.

4. Experimental section

4.1. Materials and characterization

All palladium-mediated cross-coupling reactions were performed under a nitrogen gas atmosphere in oven-dried pressure tubes. Anhydrous tetrahydrofuran (THF) and toluene were freshly distilled over sodium prior to use. All the reactions were monitored by analytical thin layer chromatography (TLC) using commercial aluminum sheets pre-coated with silica gel. Chromatography was conducted on silica gel (Acme, Mumbai, 60–120 mesh). All the commercial chemicals were used as received. The starting materials, viz. bimesityl, diiodobimesityl, and 3,3′-bis(4-formylphenyl)bimesityl were synthesized according to the earlier reported procedures established in our laboratories;[16] *p-tert*-butylphenyltetrazole **3**[24] and *p*-mesitylbenzonitrile[25]—the precursor for **4**—were synthesized according to the literature known protocol.[24,25] The detailed synthetic procedures for preparing **1** and **2** are given below (cf. Scheme 1). ^{1}H and ^{13}C NMR spectra were recorded on Bruker (500 MHz) spectrometer in $CDCl_3$ as a solvent. Chemical shifts are reported in δ-scale downfield from tetramethylsilane. The FAB-mass spectra were recorded on Jeol SX-102/mass system using argon/xenon as the FAB gas in a linear mode with *m*-nitrobenzyl alcohol as a matrix. The high-resolution ESI-mass spectra were recorded on Waters Q-TOF mass spectrometer. The elemental analyses were performed on a Thermoquest CE (EA1110) elemental analyzer. TGA and DSC analyses were carried out using a Perkin–Elmer instrument (DSC-7) at 10 °C/min under a nitrogen gas atmosphere. UV–vis absorption spectra were recorded using a Jasco-550 spectrophotometer. Photoluminescence spectra were recorded with Spex Fluolog-2 spectrofluorimeter. The UV–vis absorption, photoluminescence, and phosphorescence spectra were recorded using the spectral grade solvents. The ionization potentials were calculated by photoelectron spectroscopy (Riken Keiki, AC2) with UV intensity of 50 nW.

4.2. Synthetic procedure

*4.2.1. Preparation of p-mesitylphenyltetrazole (**4**).* To a solution of *p*-mesitylbenzonitrile[25] (5.0 g, 22.6 mmol) in 20.0 mL of DMF were added NaN_3 (2.2 g, 33.9 mmol) and NH_4Cl (1.8 g, 33.9 mmol) and the reaction mixture was heated at 120 °C. The turbid solution became clear in 5 h. The heating was continued for further 18 h, the reaction mixture was cooled and poured into ice. Resulting solid was filtered and washed with $CHCl_3$ to obtain **4** as a pure colorless solid in 86% yield, mp 271–274 °C: IR (KBr, cm^{-1}) 3003, 2948, 2860, 1635, 1452, 837; ^{1}H NMR ($CDCl_3$, 500 MHz) δ 1.97 (s, 6H), 2.33 (s, 3H), 6.95 (s, 2H), 7.27 (d, J=8.25 Hz, 2H), 7.72 (d, J=8.25 Hz, 4H); ^{13}C NMR ($CDCl_3$, 125 MHz) δ 20.8, 21.2, 110.7, 119.2, 121.5, 128.5, 130.4, 132.4, 137.7, 146.5, 155.4.

4.2.2. Preparation of 3,3′-bis(4-carboxylphenyl)bimesityl. To a solution of 3,3′-bis(4-formylphenyl)bimesityl[16c] (3.0 g, 6.7 mmol) in 30 mL of DMF and 15 mL of CH_2Cl_2 and oxone ($KHSO_5$) (8.3 g, 13.4 mmol) was added. The reaction mixture was stirred at room temperature for 3 h, solvent removed under reduced pressure, acidified with 10% HCl, and extracted with ethyl acetate. The combined extracts were washed with water, dried over Na_2SO_4, and concentrated. The pure 3,3′-bis(4-carboxylphenyl)bimesityl was obtained as a colorless solid after recrystallization from 20:80 ethyl acetate and petroleum ether mixture, yield 96%, mp 278–282 °C: IR (KBr, cm^{-1}) 3003, 2918, 2820, 1706; ^{1}H NMR (DMSO-d_6, 500 MHz) δ 1.49 (s, 6H), 1.85 (s, 6H), 1.97 (s, 6H), 7.08 (s, 2H), 7.21–7.25 (m, 4H), 7.95–7.99 (m, 4H); ^{13}C NMR (DMSO-d_6, 125 MHz) δ 18.2, 20.2, 20.9, 129.6, 129.8, 130.1, 132.1, 132.8, 133.8, 134.7, 138.0, 139.3, 146.3, 167.8; FABMS M^+ 478.21.

*4.2.3. Preparation of oxadiazole (**1**).* 3,3′-Bis(4-carboxylphenyl) bimesityl (1.5 g, 3.2 mmol) was reacted with an excess amount of $SOCl_2$ (ca. 5 mL). The unreacted thionyl chloride was first removed and the volatiles were removed in vacuo at 50 °C. The resulting acid chloride was taken to the next step immediately without further purification. To 3,3′-bis(4-chlorocarbonylphenyl)bimesityl obtained above was added *p-tert*-butylphenyltetrazole (**3**) (1.9 g, 9.4 mmol) in pyridine (15 mL) drop-wise under constant stirring. The whole of the solution was heated at 110 °C for a period of 6 h under a nitrogen gas atmosphere; during the stirring, a white precipitate gradually appeared. The reaction mixture was subjected to silica gel column chromatography using 10% ethyl acetate in $CHCl_3$ as an eluent to afford compound **1** as a colorless solid in 82% yield, mp 302–305 °C: IR (KBr, cm^{-1}) 2955, 2859, 1602, 1551, 1483, 1449; ^{1}H NMR ($CDCl_3$, 500 MHz) δ 1.37 (s, 18H), 1.65 (s, 6H), 1.97 (s, 6H), 2.06 (s, 6H), 7.09 (s, 2H), 7.33–7.38 (m, 4H), 7.56 (d, J=8.25 Hz, 4H), 8.08 (d, J=8.25 Hz, 4H), 8.18–8.22 (m, 4H); ^{13}C NMR ($CDCl_3$, 125 MHz) δ 18.0, 20.1, 20.9, 31.2, 35.2, 121.2, 122.4, 126.2, 126.9, 127.2, 129.2, 130.4, 133.2, 134.1, 135.1, 138.2, 138.9, 145.8, 155.5; HRMS (ESI-MS) *m*/*z* calcd for $C_{54}H_{54}N_4O_2$ 790.4325, found 791.4324 (M+1). Anal. Calcd for $C_{54}H_{54}N_4O_2$: C, 81.99; H, 6.88; N, 7.08. Found: C, 81.42; H, 6.78; N, 7.04.

*4.2.4. Preparation of oxadiazole (**2**).* This compound was synthesized using *p*-mesitylphenyltetrazole following the procedure used above for the preparation of oxadiazole, **1**, 87% yield, mp 315–320 °C: IR (KBr, cm^{-1}) 3028, 2963, 2867, 1617, 1494; ^{1}H NMR ($CDCl_3$, 500 MHz) δ 1.65 (s, 6H), 1.74 (s, 6H), 1.97 (s, 6H), 2.06 (s, 6H), 2.45 (s, 12H), 7.09 (s, 6H), 7.34–7.38 (m, 8H), 8.04 (d, J=8.25 Hz, 4H), 8.18–8.22 (m, 4H); ^{13}C NMR ($CDCl_3$, 125 MHz) δ 17.9, 20.1, 20.9, 21.3, 121.2, 122.4, 126.2, 126.9, 127.1, 127.2, 129.3, 130.0, 130.1, 130.4, 133.0, 133.9, 135.0, 135.2, 138.1, 138.9, 148.9, 155.5; HRMS (ESI-MS) *m*/*z* calcd for $C_{64}H_{58}N_4O_2$ 914.46333, found 915.4642 (M+1). Anal. Calcd for $C_{64}H_{58}N_4O_2$: C, 83.99; H, 6.39; N, 6.12. Found: C, 84.40; H, 6.39; N, 6.18.

4.3. Optical measurements

UV–vis absorption spectra were recorded using ca. 10^{-5} M solutions in chloroform. Fluorescence measurements were performed on dilute solutions (ca. 10^{-6} M) in chloroform and emission spectrum in each case was obtained at $\lambda_{ex}=\lambda_{max}$ (abs) with $A_{\lambda ex}\leq 0.1$ to minimize internal absorption. All absorption and fluorescence spectral recordings were performed at 25 °C (298 K). The phosphorescence spectrum was measured at 77 K in 2-methyltetrahydrofuran. Solvents used were of spectroscopic grade.

4.4. Device fabrication and characterization of PHOLEDs

The multilayer PHOLEDs were fabricated by employing the bimesitylene-based oxadiazoles **1** and **2** as host emitting materials. The ITO-coated glass substrates (Merck Display Technology, Taiwan) with a sheet resistance of $<50\,\Omega$ per square were cleaned sequentially in an ultrasonicator using acetone, detergent solution, deionized water, ethanol, 2-propanol, and then subjected to oxygen plasma and UV treatments.

4.5. Vacuum deposition

Vacuum deposition of the organic materials such as NPB, **1** or **2**, Ir(PPy)$_3$, Alq$_3$/TPBI, LiF, and Al was carried out under a pressure of 10^{-6} Torr on top of etched ITO glass substrates sequentially. The rate of deposition for organic materials was maintained in the range 0.1–0.5 Å/s. The evaporation rate and thickness of the organic layers were monitored by a quartz oscillator. After the vacuum deposition, the devices were sealed in an inert atmosphere glove box. EL spectra of the devices were obtained using a diode-array rapid analyzer system.

4.6. Electrophosphorescence measurements

Current voltage and light intensity measurements were done on a Keithley 2400 Source meter and a Newport 1835C Optical meter equipped with a Newport 818-ST silicon photodiode, respectively. The device was placed close to the photodiode such that all the forward light entered the photodiode. The effective size of the emitting diode was 4.0 mm^2, which is significantly smaller than the active area of the photodiode detector, a condition known as ‘under-filling’, satisfying the measurement protocol.[26] The EL spectra were recorded using Hitachi F-4500 spectrofluorimeter by blocking the incident radiation. The Commission Internationale de l’Eclairage (CIE) coordinates of the devices were measured by a PR650 spectroscan spectrometer.

Acknowledgements

J.N.M. is thankful to the Department of Science and Technology (DST), India for generous financial support. P.N. is grateful to UGC for a senior research fellowship. We are thankful to Prof. Shih-Sheng Sun for his generous help with the phosphorescence spectra.

Supplementary data

^{1}H and ^{13}C NMR scans and mass spectra for the intermediates and final compounds **1** and **2**. Supplementary data associated with this article can be found in the online version, at doi:10.1016/j.tet.2012.05.101.

References and notes

1. (a) *Highly Efficient OLEDs with Phosphorescent Materials*; Yersin, H., Ed.; Wiley-VCH: Weinheim, Germany, 2008; (b) Tao, Y.; Yang, C.; Qin, J. *Chem. Soc. Rev.* **2011**, *40*, 2943; (c) Chaskar, A.; Chen, H.-F.; Wong, K.-T. *Adv. Mater.* **2011**, *23*, 3876; (d) Xiao, L.; Chen, Z.; Qu, B.; Luo, J.; Kong, S.; Gong, Q.; Kido, J. *Adv. Mater.* **2011**, *23*, 926.
2. (a) Baldo, M. A.; O’Brien, D. F.; You, Y.; Shoustikov, A.; Sibley, S.; Thompson, M. E.; Forrest, S. R. *Nature* **1998**, *395*, 151; (b) Baldo, M. A.; Lamansky, S.; Burrows, P. E.; Thompson, M. E.; Forrest, S. R. *Appl. Phys. Lett.* **1999**, *75*, 4; (c) Adachi, C.; Baldo, M. A.; Thompson, M. E.; Forrest, S. R. *J. Appl. Phys.* **2001**, *90*, 5048.
3. (a) Holmes, R. J.; Forrest, S. R.; Tung, Y.-J.; Kwong, R. C.; Brown, J. J.; Garon, S.; Thompson, M. E. *Appl. Phys. Lett.* **2003**, *82*, 2422; (b) Tanaka, I.; Tabata, Y.; Tokito, S. *Chem. Phys. Lett.* **2004**, *400*, 86.
4. (a) Brunner, K.; van Dijken, A.; Börner, H.; Bastiaansen, J. J. A. M.; Kiggen, N. M. M.; Langeveld, B. M. W. *J. Am. Chem. Soc.* **2004**, *126*, 6035; (b) Wong, K. T.; Chen, Y.-M.; Lin, Y.-T.; Su, H. C.; Wu, C.-C. *Org. Lett.* **2005**, *7*, 5361; (c) Chen, Y.-C.; Huang, G. S.; Hsiao, C.-C.; Chen, S.-A. *J. Am. Chem. Soc.* **2006**, *128*, 8549; (d) Whang, D. R.; You, Y.; Kim, S. H.; Jeong, W.-I.; Park, Y.-S.; Kim, J.-J.; Park, S. Y. *Appl. Phys. Lett.* **2007**, *91*, 233501; (e) Sasabe, H.; Pu, Y.-J.; Nakayama, K.-i.; Kido, J. *Chem. Commun.* **2009**, 6655.
5. (a) Ren, X.; Li, J.; Holmes, R. J.; Djurovich, P. I.; Forrest, S. R.; Thompson, M. E. *Chem. Mater.* **2004**, *16*, 4743; (b) Shih, P.-I.; Chien, C.-H.; Chuang, C.-Y.; Shu, C.-F.; Yang, C.-H.; Chen, J.-H.; Chi, Y. *J. Mater. Chem.* **2007**, *17*, 1692; (c) Xiao, L.; Su, S.-J.; Agato, Y.; Lan, H.; Kido, J. *Adv. Mater.* **2009**, *21*, 1.
6. (a) Vecchi, P. A.; Padmaperuma, A. B.; Qiao, H.; Sapochak, L. S.; Burrows, P. E. *Org. Lett.* **2006**, *8*, 4211; (b) Sapochak, L. S.; Padmaperuma, A. B.; Cai, X.; Male, J. L.; Burrows, P. E. *J. Phys. Chem. C* **2008**, *112*, 7989.
7. Adachi, C.; Baldo, M. A.; Forrest, S. R.; Thompson, M. E. *Appl. Phys. Lett.* **2000**, *77*, 904.
8. Chen, H.-F.; Yang, S.-J.; Tsai, Z.-H.; Hung, W.-Y.; Wang, T.-C.; Wong, K.-T. *J. Mater. Chem.* **2009**, *19*, 8112.
9. Ahmed, E.; Earmme, T.; Jenekhe, S. A. *Adv. Funct. Mater.* **2011**, *21*, 3889.
10. Shih, P.-I.; Chien, C.-H.; Wu, F.-I.; Shu, C.-F. *Adv. Funct. Mater.* **2007**, *17*, 3514.
11. Holder, E.; Langeveld, B. M. W.; Schubert, U. S. *Adv. Mater.* **2005**, *17*, 1109.
12. (a) Tao, Y.; Wang, Q.; Yang, C.; Wang, Q.; Zhang, Z.; Zou, T.; Qin, J.; Ma, D. *Angew. Chem., Int. Ed.* **2008**, *47*, 8104; (b) Zheng, L.; Lee, TY.-H.; Merkel, P. B.; Chen, S. H. *J. Mater. Chem.* **2009**, *19*, 8772; (c) Tao, Y.; Wang, Q.; Ao, L.; Zhong, C.; Qin, J.; Yang, C.; Ma, D. *J. Mater. Chem.* **2010**, *20*, 1759; (d) Tao, Y.; Wang, Q.; Yang, C.; Zhong, C.; Qin, J.; Ma, D. *Adv. Funct. Mater.* **2010**, *20*, 2923; (e) Gong, S.; Chen, Y.; Luo, J.; Yang, C.; Zhong, C.; Qin, J.; Ma, D. *Adv. Funct. Mater.* **2011**, *21*, 1168.
13. (a) Leung, M.-K.; Yang, C.-C.; Lee, J.-H.; Tsai, H.-H.; Lin, C.-F.; Huang, C.-Y.; Su, Y. O.; Chiu, C.-F. *Org. Lett.* **2007**, *9*, 235; (b) Chen, S.; Xu, X.; Liu, Y.; Qiu, W.; Yu, G.; Sun, X.; Zhang, H.; Qi, T.; Lu, K.; Gao, X.; Liu, Y.; Zhu, D. *J. Mater. Chem.* **2007**, *17*, 3788.
14. (a) Wang, C.; Jung, G.-Y.; Hua, Y.; Pearson, C.; Bryce, M. R.; Petty, M. C.; Batsanov, A. S.; Goeta, A. E.; Howard, J. A. K. *Chem. Mater.* **2001**, *13*, 1167; (b) Ichikawa, M.; Kawaguchi, T.; Kobayashi, K.; Miki, T.; Furukawa, K.; Koyama, T.; Taniguchi, Y. *J. Mater. Chem.* **2006**, *16*, 221; For reviews, see: (c) Kulkarni, A. P.; Tonzola, C. J.; Babel, A.; Jenekhe, S. A. *Chem. Mater.* **2004**, *16*, 4556; (d) Hughes, G.; Bryce, M. R. *J. Mater. Chem.* **2005**, *15*, 94; (e) Shirota, Y.; Kageyama, H. *Chem. Rev.* **2007**, *107*, 953.
15. (a) Mitschke, U.; Baeuerle, P. *J. Mater. Chem.* **2000**, *10*, 1471; (b) Strohriegl, P.; Grazulevicius, J. V. *Adv. Mater.* **2002**, *14*, 1439.
16. (a) Moorthy, J. N.; Venkatakrishnan, P.; Natarajan, P.; Huang, D.-F.; Chow, T. J. *J. Am. Chem. Soc.* **2008**, *130*, 17320; (b) Moorthy, J. N.; Venkatakrishnan, P.; Huang, D.-F.; Chow, T. J. *Chem. Commun.* **2008**, 2146; (c) Moorthy, J. N.; Venkatakrishnan, P.; Natarajan, P.; Lin, Z.; Chow, T. J. *J. Org. Chem.* **2010**, *75*, 2599; (d) Moorthy, J. N.; Natarajan, P.; Venkatakrishnan, P.; Huang, D.-F.; Chow, T. J. *Org. Lett.* **2007**, *9*, 5215.
17. Cousin, D.; Mann, J.; Nieuwenhuyzen, M.; van den Berg, H. *Org. Biomol. Chem.* **2006**, *4*, 54.
18. (a) Travis, B. R.; Sivakumar, M.; Hollist, G. O.; Borhan, B. *Org. Lett.* **2003**, *5*, 1031; (b) Moorthy, J. N.; Natarajan, R.; Venugopalan, P. *J. Org. Chem.* **2005**, *70*, 8568.
19. (a) Inomata, H.; Goushi, K.; Masuko, T.; Konno, T.; Imai, T.; Sasabe, H.; Brown, J. J.; Adachi, C. *Chem. Mater.* **2004**, *16*, 1285; (b) Tsai, M.-H.; Hong, Y.-H.; Chang, C.-H.; Su, H.-C.; Wu, C.-C.; Matoliukstyte, A.; Simokaitiene, J.; Grigalevicius, S.; Grazulevicius, J. V.; Hsu, C.-P. *Adv. Mater.* **2007**, *19*, 862; (c) Kang, J.-W.; Lee, D.; Park, H.-D.; Kim, J. W.; Jeong, W.-I.; Park, Y.-S.; Lee, S.-H.; Go, K.; Lee, J.-S.; Kim, J.-J. *Org. Electron.* **2008**, *9*, 452.
20. (a) Shirota, Y.; Kuwabara, Y.; Inada, H.; Wakimoto, T.; Nakada, H.; Yonemoto, Y.; Kawami, S.; Imai, K. *Appl. Phys. Lett.* **1994**, *65*, 807; (b) Baldo, M. A.; Forrest, S. R. *Phys. Rev. B* **2000**, *62*, 10958.
21. (a) Su, S.-J.; Takahashi, Y.; Chiba, T.; Takeda, T.; Kido, J. *Adv. Funct. Mater.* **2009**, *19*, 1; (b) Kwon, S.; Wee, K.-R.; Kim, A.-L.; Kang, S. O. *J. Phys. Chem. Lett.* **2010**, *1*, 295.
22. (a) Gao, Z.; Lee, C. S.; Bello, I.; Lee, S. T.; Chen, R.-M.; Luh, T.-Y.; Shi, J.; Tang, C. W. *Appl. Phys. Lett.* **1999**, *74*, 865; (b) Shih, H. T.; Lin, C.-H.; Shih, H.-H.; Cheng, C.-H. *Adv. Mater.* **2002**, *14*, 1409; (c) Ko, C.-W. K.; Tao, Y.-T.; Lin, J. T.; Thomas, K. R. J. *Chem. Mater.* **2002**, *14*, 357.
23. Kondakova, M. E.; Pawlik, T. D.; Young, R. H.; Giesen, D. J.; Kondakov, D. Y.; Brown, C. T.; Deaton, J. C.; Lenhard, J. R.; Klubek, K. P. *J. Appl. Phys.* **2008**, *104*, 094501.
24. Wong, K. T.; Ku, S.-Y.; Cheng, Y. M.; Lin, X.-Y.; Hung, Y.-Y.; Pu, S. C.; Chou, P. T.; Lee, G. H.; Peng, S. M. *J. Org. Chem.* **2006**, *71*, 456.
25. Ueda, M.; Saitoh, A.; Oh-tani, S.; Miyaura, N. *Tetrahedron* **1998**, *54*, 13079.
26. Forrest, S. R.; Bradley, D. D. C.; Thompson, M. E. *Adv. Mater.* **2003**, *15*, 1043.